Spin Phonon Induced Collinear Order and Magnetization Plateaus in Triangular and Kagome Antiferromagnets: Applications to $CuFeO_2$

Fa Wang and Ashvin Vishwanath

Department of Physics, University of California, Berkeley, California 94720, USA
Materials Sciences Division, Lawrence Berkeley National Laboratory, Berkeley, California 94720, USA

(Received 1 November 2007; published 20 February 2008)

We study the effect of spin-lattice coupling on triangular and kagome antiferromagnets and find that even moderate couplings can induce complex *collinear* orders. On coupling classical Heisenberg spins on the triangular lattice to Einstein phonons, a rich variety of phases emerge including the experimentally observed four sublattice state and the five sublattice 1/5th plateau state seen in the magnetoelectric material $CuFeO_2$. Also, we predict magnetization plateaus at 1/3, 3/7, 1/2, 3/5, and 5/7 at these couplings. Strong spin-lattice couplings induce a striped collinear state, seen in α-$NaFeO_2$ and $MnBr_2$. On the kagome lattice, moderate spin-lattice couplings induce collinear order, but an extensive degeneracy remains.

DOI: 10.1103/PhysRevLett.100.077201 PACS numbers: 75.10.Hk, 75.80.+q

Frustrated magnets, in which classical ground states have multiple accidental degeneracies, have been at the focus of renewed attention. While much theoretical work has focused on the lifting of this degeneracy by thermal or quantum fluctuations (''order by disorder'' [1]), alternate mechanisms might dominate in real materials. One mechanism that is always present is the coupling of magnetism to the lattice (spin-phonon coupling). Such couplings lead to new theoretical problems and can induce multiferroic behavior with potentially important applications [2]. Indeed, the interaction between spin, lattice, and orbital degrees of freedom is central to understanding correlated materials [3]. Previous studies have highlighted the role of lattice distortions in promoting valence bond physics (spin Pierels effect) [4,5] in frustrated magnets. In the opposite limit of large (semiclassical) spins, the lattice coupling induced stabilization of *collinear* ground states in pyrochlore magnets was emphasized [6]. Further selection of a unique collinear ground by specific spin-phonon interactions have also been proposed [7,8].

Here we will study the effect of spin-phonon interactions on the ground states of the triangular and kagome magnets, in the classical limit. In contrast to the previously studied pyrochlore magnets, all ground states of the nearest neighbor antiferromagnets on these lattices are noncollinear (120°) configurations. We show that physically reasonable values of spin-lattice coupling can induce *collinear* orders with complex structure. Thus, even with full spin rotation invariance, collinear ground states can arise on these lattices. We believe this to be the origin of the puzzling collinear magnetism seen in triangular lattice magnets, such as $CuFeO_2$ [9], and perhaps also α-$NaFeO_2$ [10], and $MnBr_2$ [11]. In these materials with $S = 5/2$ filled shell moments, magnetic anisotropy is likely to be (and in some cases known to be) very small, and cannot be invoked to explain the collinear order. Furthermore, we study the precise pattern of the order induced within the Einstein Site Phonon (ESP) model [8], which is parameterized by a single coupling constant. The zero temperature phase diagram of the classical spin models are establish by combining analytic arguments with numerical calculations (simulated annealing). On the triangular lattice, increasing the spin-phonon coupling induces a transition from the 120° state to a collinear state with four sublattice zigzag order (Z state). The phase diagram in a magnetic field is remarkably complex, with magnetization plateaus at 1/5th, 1/3rd, 3/7th, 3/5th, 5/7th, and 1/2 of the total magnetization appearing at these couplings.

Remarkably, in $CuFeO_2$, [9] an extensively studied triangular magnet, the Z state is observed at low temperatures, which on application of a field yields a 1/5th magnetization plateau with precisely the structure obtained in our model. This was previously rather mysterious since the only available models which captured such orders were Ising Hamiltonians with large and very specific second and third-neighbor interactions ($J_2 = 0.45J_1$, $J_3 = 0.75J_1$) [12,13]. Such Ising models are unnatural given the nearly isotropic magnetic susceptibility observed in the paramagnetic state [14]. In contrast, our model is spin isotropic and involves a single parameter—the spin-phonon coupling—set at a physically reasonable value. Predictions for higher magnetization plateaus and signatures of spin-phonon coupling in this material are made. The magnetically induced electrical polarization observed in this system is however not captured by our simple model, pointing to the role of other interactions.

On the kagome lattice too we find that beyond a critical coupling, collinear ground states are obtained, but in contrast to the triangular lattice, the manifold of these states has an extensive entropy. Only at larger couplings is there a transition into a unique ground state. This may be of relevance to the recently studied kagome staircase compound, $Mn_3V_2O_8$ [15].

Spin-phonon model.—Spin-phonon couplings arise from the dependence of the exchange coupling on separation between the magnetic ions $J(r)$. Thus,

$$H = J\sum_{\langle ij\rangle}\left(1 - \alpha\frac{u_{ij}}{d}\right)\vec{S}_i \cdot \vec{S}_j + H_{\text{lattice}}(\{\vec{u}_i\}) \qquad (1)$$

where $\vec{u}_i$ is the displacement of site i and hence $u_{ij} = (\vec{u}_i - \vec{u}_j)\cdot\hat{e}_{ij}$ is the change in length of the bond ij ($\hat{e}_{ij}$ is the unit vector from site i to j), the lattice constant is d and $\alpha = dJ^{-1}\partial J/\partial r$. Two types of phonon Hamiltonians, H_{lattice}, have been proposed. First, the bond phonon model of Penc *et al.* [6], where u_{ij} are treated as independent variables and $H_{\text{lattice}} = (K/2)\sum_{\langle ij\rangle}u_{ij}^2$. Integrating out the phonons generates just the biquadratic term $-b\bar{J}\sum_{\langle ij\rangle}(\vec{S}_i \cdot \vec{S}_j)^2$. (The phonon's dynamics can be neglected if its frequency is much larger than magnetic energy scales). For large b, collinear states result, but the model is highly degenerate and selection by quantum fluctuations may be important. However, this model assumes that bond displacements are independent, which is an oversimplification for many lattices. Instead, here we turn to the second model, the ESP model of Bergman *et al.* [8] which respects the inevitable correlations between bond lengths and assumes a dispersionless optical phonon branch, $H_{\text{lattice}} = (K/2d^2)\sum_i \vec{u}_i^2$.

More realistic phonon models with multiple branches and acoustic phonons could generate complex longer-range effective spin interactions. In the interests of simplicity and generality we will restrict attention to the ESP model. Integrating out the lattice displacement $\vec{u}_i$ results in the effective spin Hamiltonian:

$$H_{\text{ESP}} = J\left[\sum_{\langle ij\rangle}\vec{S}_i \cdot \vec{S}_j - cS^2\sum_i \vec{F}_i^2\right] \qquad (2)$$

where S is the classical spin length, $c = \alpha^2 JS^2/(2K)$ is a dimensionless coupling and we have defined the dimensionless "force" on site i as $\vec{F}_i = \sum_{j\in\text{nbrs. of } i}(\vec{S}_i \cdot \vec{S}_j)\hat{e}_{ij}/S^2$. We will sometimes use the scaled coupling $\bar{J} = S^2 J$. The spin-phonon interaction seeks to *maximize* the force $\vec{F}$. Note, the second term in Eqn. (2) generates interactions involving three adjacent spins $\hat{e}_{ij}\cdot\hat{e}_{jk}(\vec{S}_i \cdot \vec{S}_j)(\vec{S}_j \cdot \vec{S}_k)$.

Triangular lattice.—In the following we will consider a single triangular lattice sheet governed by the Hamiltonian in Eqn. (2), i.e., with nearest neighbor antiferromagnetic interactions and the spin-phonon term. We focus on the zero temperature phase diagram, as a function of the single parameter c and subsequently in an applied magnetic field. Since we are primarily interested in large spin (e.g., $S = 5/2$), we focus on classical spins, where we can write $\vec{S}_i = S\hat{n}_i$, where $\hat{n}_i$ is a unit vector. If, for a moment, we restrict to only Ising states, $\vec{S}_i = \sigma_i S\vec{n}$, this effective spin Hamiltonian simplifies to an Ising model with nearest-, second-, and third-neighbor coupling, $\bar{J}(1-c)$, $c\bar{J}$ and $c\bar{J}$, respectively. However, in this model the second and third-neighbor couplings are constrained to be strictly equal. This might be a rationalization for the success of Ising models with large second and third-neighbor couplings used in previous work [12].

Consider the classical ground state on raising c. While at $c = 0$ the the regular 120° pattern of O(3) spins on the triangular lattice is realized, this is expected to survive to finite c as well. The ground state energy per site is $E_0/\bar{J} = -3/2$, and since the force vanishes in this state, it is independent of c. While a full numerical solution is required (and provided below) for the phase diagram of this model, we begin with analytic arguments which will be confirmed by the numerics. Clearly, collinear states are preferred for large c since they give rise to the maximum force. However, near the phase boundary with the 120° states, the exchange J will presumably be important, and hence we restrict attention to those collinear states that best satisfy J. These are just the ground states of the triangular lattice Ising antiferromagnet (TLIA) with nearest neighbor exchange, with two (one) up and one (two) down spins per triangle. The question of which configuration within this manifold optimizes the force term can be rigorously answered—it is the Z state. The proof is as follows. Using the dimer representation of the TLIA states, where a dimer is drawn orthogonal to each unsatisfied bond, and leads to a hard core dimer configuration on the honeycomb lattice, we see that the force on site i is determined by the dimer configurations on the hexagon surrounding site i. The force is $|\vec{F}_i| = 2$ if there is one dimer in the hexagon *or* two not-opposite dimers; otherwise $|\vec{F}_i| = 0$. The ground state maximizes $\sum_i \vec{F}_i^2$. Hence it must have two dimers in *every* hexagon (since on average there are two dimers per hexagon, having a one dimer hexagon implies also a hexagon with three dimers, which experiences no force). Combining this with the condition that the two dimers cannot be on opposite sides leads us uniquely to the Z state shown in Fig. 1.

The full phase diagram is obtained using simulated annealing on lattices with periodic boundary condition and various sizes up to 10×10, and choosing the state with lowest energy per site. Simulations on each size were done by an exponential annealing schedule from $\beta J = 0.1$ with a random initial state to $\beta J = 1000$, with a total of

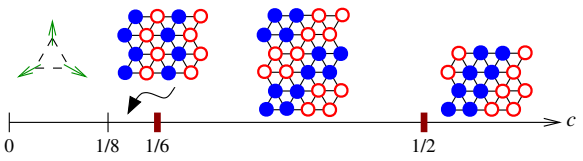

FIG. 1 (color online). Zero-field phase diagram of the triangular lattice ESP model. On increasing the spin-phonon coupling c, the 120° state is followed first by the zigzag Z state, then an 8 sublattice state and finally the stripe S state. Accidental degeneracies (thick red ticks) only occur at the phase boundaries $c = 1/6,\ 1/2$. Solid blue (hollow red) circles are up (down) spins.

20 000–40 000 sweeps, the whole process was repeated 10 times to ensure stability of results. Site update with Metropolis dynamics was used. While the algorithm does not guarantee convergence to the ground state we nevertheless believe an accurate picture emerges since all analytic expectations have been met, and we have not been able to guess ground states with better energies.

The numerically obtained phase diagram in zero field [i.e., Eq. (2)] is shown in Fig. 1. At $c = 1/8$ the 120° state is replaced by the four sublattice Z state, with alternating zigzags of up and down spins and ground state energy per spin $E_0/\bar{J} = -1 - 4c$. Beyond $c = 1/6$, an 8 sublattice state ($E_0/\bar{J} = -10c$) takes over. At $c = 1/2$, the S state of up-up-down-down stripes ($E_0/\bar{J} = 1 - 12c$) is found and persists to large couplings. At the transition points $c = 1/6$ and $c = 1/8$, there are additional accidental degeneracies, and quantum effects could be important in resolving these [16].

The phase diagram in a magnetic field $H_h = -\bar{J}h\sum_i n_i^z$ is remarkably rich (Fig. 2). For small c where the 120° state is realized, a highly degenerate set of states [17] well known for the Heisenberg triangular antiferromagnet are obtained. Since they all have vanishing force contributions, the spin-phonon interaction does not split this degeneracy. At larger values of c, the simulation shows a plethora of plateau states with collinear order, which we briefly discuss here and leave details to [16]. Interestingly the 1/5-plateau with the pattern observed in $CuFeO_2$ occur for a wide range of parameter c. For the parameter interval $0.14 < c < 1/6$ our model shows both the zigzag Z ground state at zero field and the 1/5-plateau in magnetic field, as in $CuFeO_2$. Other prominent plateaus that occur in the range of c where the Z state appears are the 3/7th and 5/7th states with 7 site unit cell, a 1/2 magnetization plateau with an 8 site unit cell and two distinct 3/5th plateaus with 5 sites per unit cell. There is also a small region of 1/3 plateau, with a 12 site unit cell. The evolution of a plateau state with increasing field can proceed in two ways—by a direct first order jump to another plateau, or by a canting transition, where the staggered moment direction moves away from the field direction. For example, the evolution of the 1/5 plateau state on increasing the field is continuous, with a gradual tilting of the staggered component away from the field. This phase boundary can be calculated analytically and agrees very well with the simulations. Such canted states are of course absent in Ising model studies [12]. Other plateaus occur for larger c, which will be discussed in detail elsewhere [16]. Amusingly, the most obvious 1/3 plateau consisting of up,up and down spins on the three sublattices, does not occur (both our 1/3 plateau have 12 spin unit cells). The 1/9th plateau extends all the way down to zero field occurs because of the accidental degeneracy at the point $c = 1/2$ which includes configurations with a maximum magnetization of 1/9th. Another consequence of accidental degeneracies is the occurrence of points in the phase diagram where four phases meet. For example the 1/3, 7/15, 1/2, 3/7 plateaus meet at a point where all four phases have exactly the same energy. These points violate the Gibbs phase rule which is based precisely on the assumption that such accidental degeneracies are absent. Introducing other interactions, as well as thermal or quantum fluctuations will resolve this degeneracy.

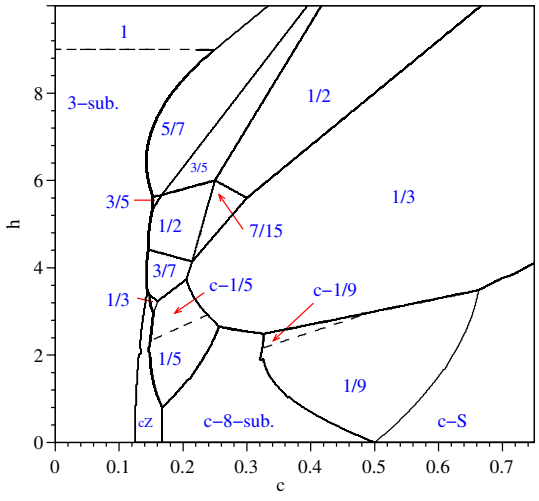

FIG. 2 (color online). $T = 0$ phase diagram of the triangular lattice ESP model. Dashed lines are continuous phase transitions, solid lines are of first order. The fraction f label magnetization plateaus, while $c - f$ are canted (noncollinear) states deriving from them; cZ is the canted Z state. The "3-sub" states at small c also occur in the pure Heisenberg model in a field.

$CuFeO_2$ *and other materials.*—In $CuFeO_2$ the 4 sublattice Z state is observed, which persists in a field upto $B < 6$ T. At higher fields $B > 14$ T, the 5 sublattice 1/5th magnetization plateau is observed. We note that both these states occur in our spin-phonon model when $0.14 < c < 1/6$. To estimate the spin-phonon coupling $c = \alpha^2\bar{J}/2K$ in $CuFeO_2$, we use $\bar{J} = 39$ K (from the measured Weiss constant [18]) and estimate $\alpha \sim 7$ and $K \sim 10\,000$ K [5], which gives $c \sim 0.1$ which is in the right ball park. The fractional lattice displacement expected is $|\vec{u}_i|/d = 2c|\vec{F}_i|/\alpha$, which is about 5% for the Z state with these parameters—although a larger value of α, arising from the sensitivity of the nearly 90° Fe-O-Fe bond to distortion or phonon anharmonicity can reduce it. While a distortion with the right symmetry has been observed [19,20], future scattering experiments should provide information regarding its size. Also, phonon softening at the M points in the Brillouin zone is expected just above the transition. Although an isotropic spin model with magnetic order cannot have a magnetization plateau centered at zero field, even a very small magnetic anisotropy (e.g., an easy axis anisotropy $-D\sum_i S_{zi}^2$) can produce the observed zero magnetization plateau, since the plateau width ΔB scales as $\Delta B \propto \sqrt{D\bar{J}}$. Even a 1% anisotropy $D/\bar{J}$ produces the right plateau width [18]. The magnetization profile as a function

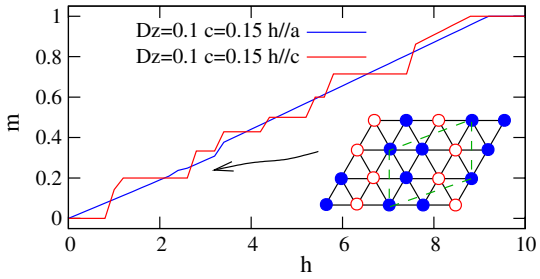

FIG. 3 (color online). Predicted magnetization (m) curve for $CuFeO_2$ with $c = 0.15$ and 10% anisotropy with field parallel (red) and perpendicular (blue) to the easy axis. Plateaus occur at $m = 0,\ 1/5,\ 1/3,\ 3/7,\ 1/2,\ 3/5,\ 5/7,\ 1$. One unit of field is $\sim$12 T. Inset: the $m = 1/5$ state.

of field at $c = 0.15$ with a somewhat larger 10% easy axis anisotropy is shown in Fig. 3 (the field scale $\bar{J}/g\mu_B S$ is $\sim$12 T) for fields parallel and perpendicular to the easy axis (c axis). These are in broad agreement with recent measurements in fields below 40 T [20]. In particular, in addition to the $1/5$th plateau a $1/3$rd plateau was observed as in our simulations. However, we predict this to be a complex 12 sublattice order, not the obvious three sublattice state that was implicitly assumed. Resolving the structure of this and higher field plateaus will allow for a test of our theory. Lastly, we note that the spiral ordered ferroelectric phase observed in the field range $7 < B < 14$ T [14] is not produced here, indicating the importance of other couplings, e.g., to the oxygen atoms mediating the superexchange interaction. The up-up-down-down stripe pattern for $1/2 < c$ is the order observed in triangular lattice compounds such as α-$NaFeO_2$, [10] and $MnBr_2$ [11]. Our model predicts a $1/9$th and $1/3$ plateaus in these materials.

Kagome lattice.—The Einstein site phonon model on the kagome is virtually identical to the triangular case, except that the lower symmetry in this case allows for an anisotropic confining potential on the atoms. For simplicity, we assume an isotropic confining potential, but the main results are independent of this assumption.

Simulated annealing was applied to this model with similar settings as the triangular case. The zero-field phase diagram is presented in Fig. 4. For small c we still get the ground states of the pure Heisenberg model, which are known to be extensively degenerate. For $c > 1/12$ we get collinear states, but in the range $1/12 < c < 1/6$ an *extensive* degeneracy remains [21]. Even more interestingly, the zero-field ground states can have arbitrary magnetization ranging from $-1/9$ to $1/9$ per site. Therefore, in this zero temperature classical model, applying a small field will immediately induce a $1/9$-magnetization-plateau state. We expect that thermal and/or quantum fluctuation can lift this accidental degeneracy which is left for future work [16].

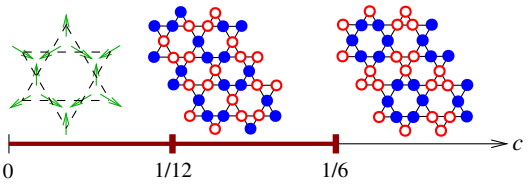

FIG. 4 (color online). Zero-field phase diagram of the ESP model on kagome lattice. Extensive degeneracy (marked red) persists into $1/12 < c < 1/6$ where collinear states occur. A representative configuration is shown in that case.

Further increasing c beyond $1/6$ pushes the system into a unique collinear states (see Fig. 4).

In conclusion, our studies suggest that spin-phonon couplings may be more widely relevant than previously believed.

We acknowledge support from LBNL No. DOE-504108 and useful discussions with K. Damle, F. Ye, D. Huse, O. Tchernyshyov, and R. Cava.

[1] C. L. Henley, Phys. Rev. Lett. **62**, 2056 (1989).
[2] Sang-Wook Cheong and Maxim Mostovoy, Nat. Mater. **6**, 13 (2007); R. Ramesh and N. Spaldin, Nat. Mater. **6**, 21 (2007).
[3] Y. Tokura and N. Nagaosa, Science **288**, 462 (2000).
[4] F. Becca and F. Mila, Phys. Rev. Lett. **89**, 037204 (2002); C. Jia and J. H. Han, Physica (Amsterdam) **378–380B**, 884 (2006).
[5] K. Kodama *et al.*, Science **298**, 395 (2002).
[6] K. Penc, N. Shannon, and H. Shiba, Phys. Rev. Lett. **93**, 197203 (2004).
[7] Oleg Tchernyshyov, R. Moessner, and S. L. Sondhi, Phys. Rev. Lett. **88**, 067203 (2002).
[8] D. L. Bergman, R. Shindou, G. A. Fiete, and L. Balents, Phys. Rev. B **74**, 134409 (2006).
[9] K. Takeda *et al.*, J. Phys. Soc. Jpn. **63**, 2017 (1994); Y. Ajiro *et al.*, J. Phys. Soc. Jpn. **64**, 3643 (1995).
[10] T. McQueen *et al.*, Phys. Rev. B **76**, 024420 (2007).
[11] T. Sato, H. Kadowake, and K. Ito, Physica (Amsterdam) **213B**, 224 (1995).
[12] M. Mekata *et al.*, J. Phys. Soc. Jpn. **62**, 4474 (1993).
[13] M. L. Plumer, Phys. Rev. B **76**, 144411 (2007).
[14] T. Kimura, J. C. Lashley, and A. P. Ramirez, Phys. Rev. B **73**, 220401(R) (2006).
[15] E. Morosan *et al.*, Phys. Rev. B **76**, 144403 (2007).
[16] F. Wang and A. Vishwanath (to be published).
[17] A. V. Chubukov and D. I. Golosov, J. Phys. Condens. Matter **3**, 69 (1991).
[18] O. Patrenko *et al.*, J. Phys. Condens. Matter **17**, 2741 (2005).
[19] F. Ye *et al.*, Phys. Rev. B **73**, 220404(R) (2006).
[20] N. Terada *et al.*, Phys. Rev. B **75**, 224411 (2007).
[21] The degeneracy is a subset of that described in A. Sen, K. Damle, and A. Vishwanath, arXiv:0706.2362.